Analysis of linearized inverse problems in ultrasound transmission imaging

H. Wang[1], H. Gemmeke[2], K. W. A. van Dongen[3], T. Hopp[2], and J. Hesser[1]

[1] *Medical Faculty Mannheim, Heidelberg University, Mannheim, Germany, E-mail: hongjian.wang@medma.uni-heidelberg.de*
[2] *Institute for Data Processing and Electronics, Karlsruhe Institute of Technology, Karlsruhe, Germany*
[3] *Faculty of Applied Sciences, Delft University of Technology, Delft, Netherlands*

Abstract

The purpose of this paper is to analyze the linearized inverse problem during the iterative solution process of the ill-posed nonlinear inverse problem of image reconstruction for ultrasound transmission imaging. We show that the conjugate gradient applied to normal equation (CGNE) method gives more reliable solutions for linearized systems than Tikhonov regularization methods. The linearized systems are more sensitive when treated by CGNE than by Tikhonov regularization methods. The Tikhonov regularization is less effective at the beginning of the outer-loop iteration, where the nonlinearity is dominating while the conjugate gradient for the linearized system stops earlier. Only when the linear approximation is good enough to describe the whole system, Tikhonov regularization can fully play its role and give slightly better reconstruction results as compared to CGNE in a very noisy case.

Keywords: Gauss-Newton method, Inverse problem, Sensitivity analysis, Tikhonov regularization, USCT

1 Introduction

Ultrasound computed tomography (USCT) as imaging method offers high potential for breast cancer diagnosis. Due to the acquisition of transmission and reflection data from current 2D or 3D USCT devices [1-4], three types of images can be reconstructed from the acquired signals: reflection, attenuation and speed of sound (SoS) images [5]. While reflection images [6, 7] reveal changes in the echo texture of the surfaces between different tissues (qualitative imaging), transmission tomography offers quantitative characterization of the imaged tissue or materials by SoS and attenuation profiles [8].

The process of transmission imaging of the USCT system at *Karlsruhe Institute of Technology* (KIT) [1, 4] is separated into two parts: a forward model approximating the path of the ultrasound wave traveling through the 3D aperture; and an inverse problem given by the forward model and the measured signals to reconstruct the image. Our forward model is based on a paraxial approximation of the wave equation [9-11], which computes the pressure field $p(\eta)$ for known complex refraction index $1+\eta$. The inverse problem is hereby formulated as a nonlinear least-squares problem

$$f(\eta) = \frac{1}{2}\|p(\eta) - \hat{p}\|_2^2 = \frac{1}{2}\|r\|_2^2, \tag{1}$$

where $r : \mathbb{C}^n \to \mathbb{C}^m$ is called *residual vector*. Here, $\hat{p} \in \mathbb{C}^m$ are the pressure fields measured at the receivers, and $p(\eta) : \mathbb{C}^n \to \mathbb{C}^m$ are the predicted pressure fields computed according to the forward model (2). By minimizing $f(\eta)$ we want to reconstruct for the SoS and attenuation parameters that are inherent in η.

For the 3D USCT system reported in [1], a number of A-scans are performed to reconstruct a volume of voxels for a breast with a diameter of about 16 cm. As the validity of the paraxial approximation for forward angles is only up to 20°, the number of usable A-scans for transmission tomography is limited to about 6%. This is the main reason that the reconstruction using the paraxial approximation is an ill-posed problem. To solve this large-scale nonlinear inverse problem, we use a Newton type method yielding a set of linearizations of the problem (1). This is a standard approach for nonlinear inverse problems [12]. Due to the ill-posed nature of the problem, regularization is necessary. We choose three common methods of regularization for solving the linearized sub-problems in an inner loop: *conjugate gradient applied to normal equation* (CGNE) [13, 14]; damped least-squares [15, 16]; and gradient magnitude. The latter two use Tikhonov regularization.

In this paper, we specifically focus on analyzing the properties of the numerical solutions of the linearized inverse problems arising from Newton type iterations, with common regularization techniques. By this analysis we aim to show how well the predicted data match the true data and how close a particular estimate of the model parameters is to the true solution. For this type of problems, we propose using standard methods for analyzing linear inverse problems by computing the data resolution and model resolution [16] at different iterations. We choose standard Tikhonov type [15] regularization methods because they have closed-form solutions in these matrices.

2 Method

2.1 Forward model

The basis for transmission tomography is the wave propagation of ultrasound including refraction, diffraction, and forward scattering which is mathematically described by the wave equation for inhomogeneous media [17]. A full solution of the wave equation is computationally highly demanding and in practice an approximation is necessary. We make the assumption of a constant density fulfilled in the soft tissue of the breast, and use the paraxial approximation [9-11] where the forward solution of frequency dependent pressure field on the computational grid can be formulated as

$$p_{z+1} = e^{i\Delta z k_0 \eta_z} \mathscr{F}^{-1}\left\{ e^{i\Delta z\sqrt{k_0^2-\xi^2}} \mathscr{F}\{p_z\}\right\}. \tag{2}$$

The acoustic medium is described by the background wave number $k_0 = \omega/c$ and the refractive index $1+\eta$, where $\omega = 2\pi f$ is the angular frequency for frequency f and spped of sound c of the background medium, and η accounts for the deviation of the inhomogeneity from the background medium. The forward solution is considered as a set of parallel slices perpendicular to the emission direction, where the index z for variables p and η denotes the considered z slice, whereas the indices for the (x,y)-directions are omitted. The spectral variable is denoted by ξ and the discrete Fourier transformation and its inverse are denoted by $\mathscr{F}$ and $\mathscr{F}^{-1}$ in 1D or 2D, depending on whether the problem is considered in 2D or 3D respectively.

2.2 Inversion by Gauss-Newton conjugate gradient

Image reconstruction estimates SoS, denoted as c, and attenuation, denoted as Δatt, which are incorporated in the complex variable η. To be specific, $\eta = a + i\frac{b}{\omega}$, where $\mathrm{Re}(\eta) = a = c_0/c - 1$ describes the deviation of c from the SoS c_0 in the background medium; and $\mathrm{Im}(\eta) = b/\omega = \Delta\mathrm{att}$ accounts for the deviation in the attenuation. We estimate η via solving the least-squares inverse problem (1) in a two-level strategy, by an outer and an inner loop. At each iteration of the outer loop, we linearize and reformulate the inverse problem using the Gauss-Newton (GN) method, which can be viewed as a modified Newton's method [18]. Specifically, given the nonlinear least-squares problem $f(\eta)$ of (1), instead of solving the standard Newton equations $\nabla^2 f(\eta) = -\nabla f(\eta)$ for a search direction d (which can be over-determined or under-determined depending on matrix dimensions), we solve the following system, i.e. the normal equations, to obtain the search direction

$$J^T J d = -J^T r. \tag{3}$$

Here, the derivatives of $f(\eta)$ are expressed in terms of the Jacobian J, which is the $m \times n$ matrix of the first partial derivatives of the residual vector, defined by

$$J = \left[\frac{\partial r_j}{\partial \eta_i} \right]_{\substack{j=1,2,\ldots,m \\ i=1,2,\ldots,n}} = \left[\nabla r_1^T, \nabla r_2^T, \ldots, \nabla r_m^T \right]^T. \tag{4}$$

The use of the approximation $\nabla^2 \approx J^T J$ relieves us to compute individual residual Hessians $\nabla^2 r_j, j = 1,2,\ldots,m$. To solve the linearized system (3), where the system matrix now corresponds to $J^T J$, we use the conjugate gradient (CG) method [19] as an inner loop solver.

2.3 Regularization

The minimization problem of the least-squares (1) is ill-posed, making regularization necessary. We analyze three methods for solving the linearized systems in the inner loop.

Method No.1: CGNE. The Gauss-Newton CG method applies CG to the normal equations of the linearized problem (3). As discussed in [13], this method has a regularization effect which comes from early termination of the iteration.

Method No.2: Damped least-squares regularization (denoted as Reg-DLS). A commonly used regularization method is *Tikhonov* regularization [15]. In our reconstruction problem, the goal is to estimate η in (2). Note that the GN search direction d in (3) is actually an update that will be added to the current guess of η at a given outer-loop iteration. If there exists an estimate of $\hat{\eta}$ that is close to the true η, then a Tikhonov regularization term can be defined to minimize the difference between $\hat{\eta}$ and the current guess. For example, let us consider η_{cur} as the best estimate so far for a given outer-loop iteration. We can simply assume $\hat{\eta} = \eta_{\text{cur}}$. Then, the regularization term for the linearized system at this outer-loop iteration is defined as

$$||\eta_{\text{new}} - \hat{\eta}||_2^2 = ||\Delta\eta||_2^2 = ||\alpha d||_2^2. \tag{5}$$

Accordingly, solving the linearized system (3) with this regularization term is equivalent to solving

$$\min_d ||Jd - r||_2^2 + \lambda^2 ||d||_2^2. \tag{6}$$

where λ is a regularization parameter. The minimizer solution d is obtained by solving

$$\left(J^T J + \lambda^2 I\right) d = J^T r. \tag{7}$$

Method No.3: Gradient magnitude regularization (denoted as Reg-GM). Another Tikhonov regularization term is based on a smoothness assumption using the discretized gradient as filter $[-1,1]$. Therefore, the regularization term is defined to penalize the gradient magnitude (GM) of η, i.e.

$$\|L\eta_{\text{new}}\|_2^2 = \|L(\eta + \alpha d)\|_2^2 \tag{8}$$

at a given outer-loop iteration, where

$$L = \begin{pmatrix} -1 & 1 & & & & \\ & -1 & 1 & & & \\ & & \dots & \dots & & \\ & & & & -1 & 1 \\ & & & & & 0 \end{pmatrix} \in \mathbb{R}^{n\times n}. \tag{9}$$

Accordingly, solving the linearized system (3) with this regularization term is equivalent to solving

$$\min_d \|Jd - r\|_2^2 + \lambda^2 \|L(\eta + d)\|_2^2. \tag{10}$$

The minimizer solution d is obtained by solving

$$\left(J^T J + \lambda^2 L^T L\right) d = J^T r - \lambda^2 L^T L\eta. \tag{11}$$

2.4 Analysis tools

We need to solve the linear inverse problem (3), or (7), or (11) at each outer-loop iteration of the reconstruction. We call d the *model parameters* and r the *data*, of the linear inverse problem $Jd = r$. Note that the term "model parameters" in the rest of this paper does NOT refer to the parameters η that we aim to reconstruct. We compute the *data resolution matrix* N and *model resolution matrix* R that are defined in [16], to respectively reflect how well the predicted data fits the observed data (via N), and how close a particular estimate of the model parameters is to the true solution (via R). In order to quantify the resolution quality, we use *Dirichlet spread functions* [16] which are based on the size, or *spread*, of the off-diagonal elements of resolution matrix. We also use the *Backus-Gilbert spread functions* [20], which is a weighted version of the spread functions.

3 Results

We compute the resolution matrices of the linearized problems arising from outer-loop iterations, when we apply different regularization methods and parameters. We simulate the measurements data of pressure field $\hat{p}$, based on the forward model of equation (2), as $p(\eta_{\text{exact}})$ plus additive Gaussian noise characterized by the signal-to-noise ratio (SNR). The known η_{exact} is the ground truth of a breast simulation. We only focus on 2D reconstruction problems, where the y dimension is omitted. The problem size n is the 2D phantom image size, i.e. $n = n_x \times n_z$, while the size of the measurements data depends on the number of transducers n_t, i.e. $m = n_x \times n_t$. For analysis purpose, at every outer-loop iteration, we have to compute, store and perform SVD or other operations on the system matrix of size $m \times n$, the data resolution matrix of size $m \times m$, and the model resolution matrix of size $n \times n$. The computational load and necessary memory are impractical for real-size problems. Therefore, we used a reduced problem setting as follows: the image size for all phantoms is $n_x \times n_z = 48 \times 36$ ($n = 1728$) with each pixel of size $\Delta z = 0.61$ mm; the radius of the measuring device is 18.2 mm and the radius of the phantom is 10.6 mm; $n_t = 128$ transducers are simulated at the frequency of 2.5 MHz. For the two Tikhonov methods Reg-DLS and Reg- GM, we set the regularization parameter λ by the L-curve method [15] applied at every outer-loop iteration. We perform an extra test for Reg-DLS with significantly larger λ values denoted as “Reg-DLS-lcurve2”.

We plot the spread values of data resolution and model resolution matrices during 50 Gauss-Newton iterations for a noisy case using data with a SNR = 40dB, as shown in Figure 1. From our results, the data matrix N is a very sparse matrix, with large values located on the main diagonal and sub-diagonal positions. This means each row has a single sharp maximum centered about the main diagonal, and the data are well resolved. This phenomenon is testified by the upper chart in Figure 1, where the CGNE method has the smallest Dirichlet spread values when compared to any other Tikhonov regularization methods. This is because the Tikhonov regularization has the effect of preventing data over-fitting, where the predicted data are weighted average values of more neighboring observed data than the CGNE method, and hence are generally more biased. This property of the Tikhonov regularization results in more non-zero elements in each row of its data matrix N, and therefore larger Dirichlet spread values.

During the first few outer-loop iterations, the linearized systems are not stable, which is reflected by the fluctuations of the Dirichlet spread curves. As the reconstruction process continues, the spread values become stable after a certain number of outer-loop iterations, meaning that the results become more reliable. The R’s Backus-Gilbert spread values from Tikhonov regularization methods also fluctuate during the first few outer-loop iterations. This indicates that the model parameters possess a bad ordering since the Backus-Gilbert spread favors a natural ordering in the model parameters, where the rows of R represent localized averaging functions [16]. However, for the parameters that we aim to reconstruct, they are mostly smooth and well-ordered, implying that the linearized approximations during

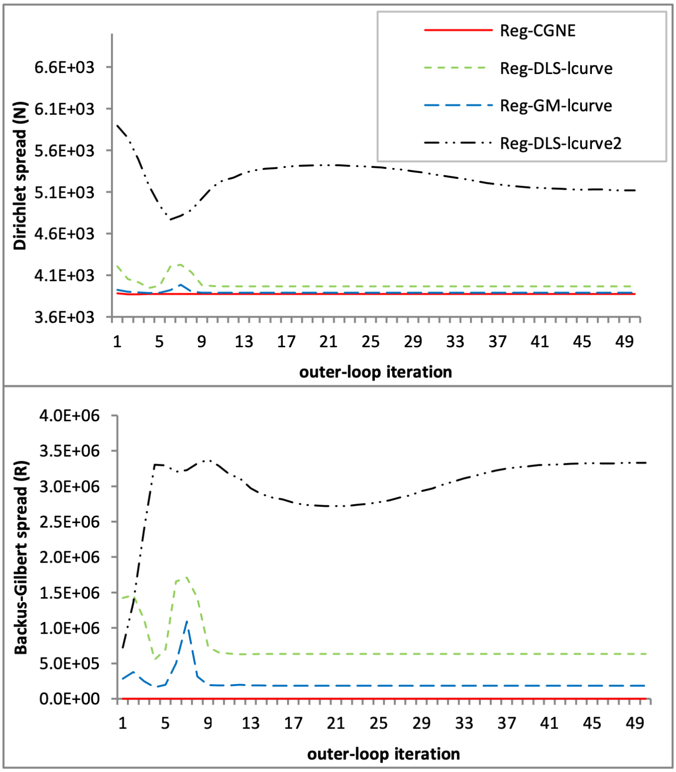

Figure 1: The spread values of data resolution and model resolution matrices during 50 Gauss-Newton iterations for noisy data with a SNR = 40 dB. The horizontal axis indicates the outer-loop iterations. **Top:** the Dirichlet spread of data resolution matrix. **Bottom:** the Backus-Gilbert spread of model resolution matrix.

the first few outer-loop iterations are not reliable. This is in agreement with our observations for the analysis of data resolution matrices.

We found that the method Reg-DLS-lcurve2 converges obviously slower than other methods. This method has the largest λ values, and therefore, the outer-loop iterative steps are more like gradient descent as compared to other methods whose steps are more like the Newton-type method. This explains the slower convergence. On the other hand, this method converges to slightly better reconstructions with our noisy data of SNR = 40dB.

4 Conclusions

We have analyzed the properties of the numerical solutions of the linearized inverse problems handled by common regularization techniques, arising from Gauss-Newton iterations in image reconstruction of ultrasound transmission tomography. To analyze the system sensitivity, we have computed the data resolution and model resolution of the linearized systems when applied to the CGNE method and to two Tikhonov regularization methods DLS and GM. Our analysis of the linear problems during the iterative solution process gives valuable information about the problem itself and yields good indications of the success of the solution process. Based on the analysis, a combination of different strategies, starting with CGNE and ending with Tikhonov would be reasonable.

References

[1] H. Gemmeke and N. V. Ruiter.: 3D Ultrasound Computer Tomography for medical imaging. NIM Nucl. Instr. & Meth. In Phys. Res. Vol. Ax (2007) 1057-65

[2] N. Duric, P. Littrup, P. Chandiwala-Mody, C. Li, S. Schmidt, L. Myc, O. Rama, L. Bey-Knight, J. Lupinacci, B. Ranger, A. Szczepanski, and E. West.: In-vivo imaging results with ultrasound tomography: Report on an ongoing study at the Karmanos Cancer Institute. Proc. SPIE vol. 7629 (2010)

[3] J. Wiskin et al.: Inverse Scattering and Refraction Corrected Reflection for Breast Cancer Imaging. Proc. SPIE vol. 7629 (2010)

[4] N. V. Ruiter, G. Göbel, L. Berger, M. Zapf, and H. Gemmeke.: Realization of an optimized 3D USCT. Proc. SPIE vol. 7968 (2011) 796805

[5] N. Ozmen, R. Dapp, M. Zapf, H. Gemmeke, N. V. Ruiter and K. W. van Dongen.: Comparing different ultrasound imaging methods for breast cancer detection. IEEE Transactions on Ultrasonics, Ferroelectrics, and Frequency Control 62(4) (2015) 637-646

[6] J. van der Neut, J. T. Fokkema, P. M. van den Berg, M. Zapf, N.V. Ruiter, U. Taskin, and K. W. A. van Dongen.: Ultrasonic synthetic-aperture interface imaging. IEEE Transactions on Ultrasonics, Ferroelectrics, and Frequency Control 66(5) (2019) 888- 897

[7] J. van der Neut, P. M. van den Berg, J. T. Fokkema and K. W. A. van Dongen.: Acoustic interface contrast imaging. Inverse Problems 34(11) (2018) 115006

[8] J. F. Greenleaf and R. C. Bahn.: Cinical imaging with transmissive ultrasonic computerized tomography. IEEE Transactions on Biomedical Engineering 28(2) (1981) 177-185

[9] H. Gemmeke et al.: Wave equation based transmission tomography. Proc. IEEE Int. Ultrason. Symp. (IUS) (2016) 1-4

[10] L. Althaus.: On acoustic tomography using paraxial approximations. M.S. thesis, Darmstadt University of Technology, Department of Mathematics, Darmstadt, Germany (2016)

[11] U. Taskin, N. Ozmen, H. Gemmeke and K. W. van Dongen.: Modeling breast ultrasound on the applicability of commonly made approximations. Archives of Acoustics 43(3) (2018) 425-435

[12] B. Kaltenbacher, A. Neubauer, and O. Scherzer.: Iterative Regularization Methods for Nonlinear Ill-Posed Problems. Radon Series on Computational and Applied Mathematics. De Gruyter (2008)

[13] M. Hanke.: Regularizing properties of a truncated newton-cg algorithm for nonlinear inverse problems. Numerical Functional Analysis and Optimization 18(9) (1997) 971-993

[14] M. Hanke.: Conjugate gradient type methods for ill-posed problems. Routledge (2017) Analysis of linearized inverse problems in ultrasound transmission imaging

[15] P. C. Hansen.: Regularization tools: A MATLAB package for analysis and solution of discrete ill-posed problems.: Numerical Algorithms 6(1) (1994) 1-35

[16] W. Menke.: Geophysical data analysis: Discrete inverse theory (MATLAB Edition). 3rd ed, Academic Press (2012)

[17] P. Suetens.: Fundamentals of medical imaging. 2nd ed. Cambridge University Press, Cambridge, UK (2009)

[18] J. Nocedal and S. Wright.: Numerical Optimization (Second Edition). Springer- Verlag New York (2006)

[19] J. R. Shewchuk.: An introduction to the conjugate gradient method without the agonizing pain. (1994)

[20] G. E. Backus and J. F. Gilbert.: Numerical application of a formalism for geophysical inverse problems. Geophys. J. Roy. Astron. Soc 13 (1967) 247-276